

# Luminescence and current–voltage characteristics of solar cells and optoelectronic devices

G. Smestad

*Hahn Meitner Institute (S), Glienicker Strasse 100, W-1000, Berlin 39, Germany*

and

H. Ries

*Paul Scherrer Institute, CH-5232 Villigen-PSI, Switzerland*

Received 9 September 1991; in revised form 23 October 1991

The transduction and conversion of light into work via a quantum process is dependent on the luminescent properties of the materials involved. Materials that can exhibit emission of light upon illumination are likely candidates for solar cells, detectors and optoelectronic devices. This radiative recombination in a material is directly related to the output device parameters, such as the current voltage characteristics. The chemical potential of the incoming light is a function of the photon energy and incident radiance. The maximum amount of work per particle, or voltage, that can be extracted by a solar converter is shown to be equal to chemical potential of the excitation, which can be inferred from the photoluminescence efficiency at ambient temperature. A discussion is made as to the use and optical properties of materials such as Si, GaAs, FeS<sub>2</sub>, and organic dyes as efficient solar cell materials. In particular, the silicon *I–V* curve and luminescence are evaluated using the model, and shown to correspond to measured devices. A discussion is also made as to the extension of the luminescence model to the understanding of the light emitting diode, or LED. By allowing the absorber to remain as thin as possible, lower recombination fluxes and higher voltages are possible in solar cells and detectors.

## 1. Introduction

Conversion of light into electricity or into chemical products in a quantum system can occur from the absorption of a photon via the formation of an excited electronic state. This excited state of the absorber material is used to produce electron–hole pairs, as in solar cell materials such as Si or GaAs, or spatially separated bound electron hole pairs, as in biological and organic materials [1–3]. In a chemical quantum system, such as photosynthesis, the excitation leads to the formation of chemical products with higher free energy than that of the starting materials [4,5]. A quantum conversion process is differentiated from thermal conversion, in which the light is converted into heat, at some temperature, before work is extracted. In contrast to a thermal system, in a quantum system, such as a

solar cell, a fixed number of photons yields one or a fixed number of energy quanta such as excited electrons. This fixed number of excitations can be counted in a way that is analogous to Dalton's law. If the interaction of light with a material produces electrons, or species in a higher energetic state, then the reverse reaction, which must also be possible, will produce light from the absorber material. This is the definition of photoluminescence, an example of which can be found using the brightly fluorescent organic dyes used in fabrics and signposts.

The usual method of characterizing a solar cell or optoelectronic is to utilize the absorption coefficient, and transport parameters, such as charge carrier mobility, and electron lifetime, of the absorber material in order to determine how many incident photons will yield electrons in the external circuit [1,2]. This technique is analogous to building a mathematical model of a car, down to the level of the gears, in order to determine the limits of its performance. Another, less popular, method that has been used to determine the potential of an absorber material to yield useful work is a more global approach [5–9]. This would be analogous to determining the Carnot efficiency as an upper limit for the performance of a car even before the details of the fabrication and configuration are determined. In this paper, a thermodynamic–quantum mechanical approach will be used to relate the luminescence or photoluminescence of a material to its ability to do work, or to produce a voltage. In contrast to previous work, discussed in section 3.2.2, the current–voltage curve, and conversion efficiency, of the quantum system will be simply described from optical measurements of: (1) absorptivity, and (2) photoluminescence efficiency. Characterization of semiconductors by measuring the photoluminescence or electroluminescence is done routinely [10,11]. In solar cell and detector applications, one often views photoluminescence as a loss of energy, rather than as a requirement for efficient conversion. In the open circuit condition, where energy is not extracted, energy dissipation by luminescence will be shown to be a measure of the device's ability to bypass other losses, in producing work from light (or vice versa in the case of the LED). It is shown that the current–voltage characteristics and luminescent radiance for a quantum system are directly connected. Indeed, the luminescence, while constituting the only unavoidable current loss, can be used to determine the voltage. By measuring the luminescence, one can therefore assess the absorber material quality, and improve optoelectronic device fabrication techniques.

## **2. Luminescent efficiency**

### *2.1. A model quantum system*

For the purposes of this paper, we shall consider the two state quantum system as outlined in fig. 1. Light is absorbed by the material to produce electrons in the conduction band, CB, which can recombine in three separate ways. Electrons can recombine radiatively, giving up the excitation energy in the form of an emitted luminescent photon [4,5,8]. The electrons can also decay non-radiatively through

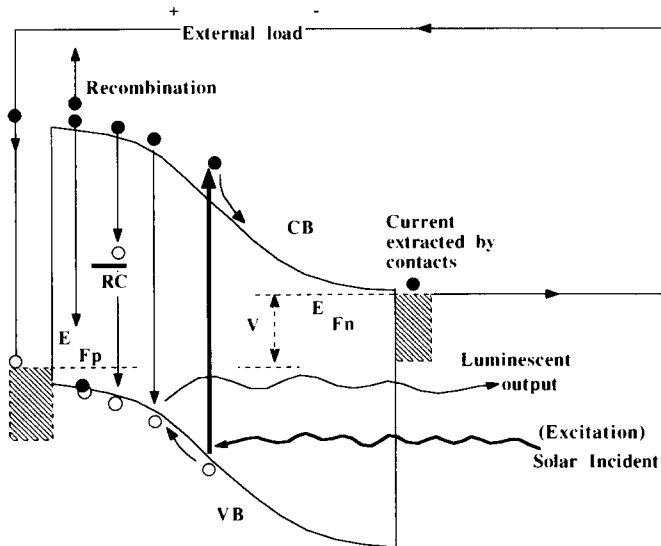


Fig. 1. A two-level quantum system connected to an external load. Solar or incident radiation produces an excitation which has three pathways for recombination. Non-radiative recombination can occur through Auger processes, or through a recombination center, RC, to produce phonons or heat. Luminescent output represents the radiative recombination. Recombination through the external load, at a voltage,  $V$ , is shown via the quasi-Fermi levels,  $E_{Fn}$  and  $E_{Fp}$ .

traps, or through Auger recombination to produce a phonon or lattice vibration [1,8]. Alternatively, if the electron survives these recombination processes, it may be collected by the external circuit to produce a voltage, and to do work, as it again returns to the ground state or valence band, VB. This voltage is simply the difference in chemical potential, between the quasi-Fermi levels,  $E_{Fn}$  and  $E_{Fp}$ , of electrons and holes in the CB and VB, as shown by the dotted lines in fig. 1 [1].

Each process in fig. 1 also implies the reverse reaction. For example, the absorption or excitation reaction implies the backward reaction, which is radiative recombination. Just as in a chemical reaction, products can recombine to produce starting materials, although these processes can occur with different rate constants. Analogous to a chemical reaction, the reaction of electrons with photons is characterized by a Gibbs free energy per particle, or chemical potential, which represents the net direction in which the reaction proceeds [12]. In the section that follows, this chemical potential will be related to luminescence and recombination. This recombination will then be balanced with the input flux in order to obtain the dependency of the voltage on the luminescence efficiency, as well as the current voltage characteristics of the device.

## 2.2. Luminescent radiance and radiative recombination

The emission of light produced from radiative recombination from a material at ambient temperature ( $T_0 = 300$  K) is given by the ideal luminescence spectrum,

which is a generalized Planck equation, corrected for the quantum emissivity,  $\epsilon$ , of the process. Thus,

$$L_x(e, \mu, T_0) = \epsilon(e) \frac{2n^2}{h^3 c^2} \frac{e^3}{\exp[(e - \mu_x)/kT_0] - 1}, \quad (1)$$

where  $e$  is the photon energy, and  $L$  is the spectral radiance, which is the radiant power per area per projected solid angle per photon energy interval. To obtain the flux or number of photons, one divides eq. (1) by the photon energy,  $e$ . The constant  $n$  is the index of refraction of the medium in which the solid angle is measured. For a silicon absorber immersed in glass or plastic, the value of  $n$  is between 1.45 and 1.6 inside the glass and 3.5 inside the silicon. The constants  $h$  and  $c$  are Planck's constant and the speed of light in vacuum, respectively. The constant  $k$  is Boltzmann's constant ( $8.62 \times 10^{-5}$  eV/K). The chemical potential, or charge times voltage, is given by  $\mu$ . The subscript  $x$  refers to the light source. In this paper, 0 will refer to ambient radiation, OR will refer to the radiative recombination, and S, or in, will refer to solar or incident radiation on the absorber. The subscript SC will refer to the absorbed or short circuit flux. Eq. (1) has the form one would expect for a Boson gas such as photons [12,13].

A black body, such as the sun, can be viewed as a special kind of luminescent body with zero chemical potential at a high temperature,  $T_s = 5762$  K. Another way of looking at eq. (1) is to consider the entropy balance during the absorption of a photon [9]. The loss of a photon from a beam of light is accompanied by a loss in entropy of  $e/T_r$ , where  $T_r$  is the temperature of the light [12]. If only  $\mu$  is converted to work at ambient temperature  $T_0$ , then  $(e - \mu)/T_0$  is the entropy transferred to the surroundings. Equating these two entropies yields eq. (1) from the more commonly described Planck black body equation. Thus, one can regard solar photons as having a chemical potential  $\mu = e(1 - T_0/T_r)$  equal to the maximum work, or free energy, they can produce at ambient temperature.

The emissivity,  $0 < \epsilon < 1$ , measures how close the material comes to the ideal case  $\epsilon = 1$ . This will now be shown to be a function of the material properties and absorber thickness. A quantity directly related to the emissivity is the absorptivity. The quantum absorptivity,  $a(e)$ , is the fraction of the incoming light which is absorbed by the material to produce an excited state. From a consideration of the detailed balance between the absorption and emission of light, it can be shown that the quantum absorptivity and emissivity are equal, just as are the thermal absorptivity and emissivity as expressed by Kirchhoff's law [5,9]. Neglecting free carrier absorption, the thermal and quantum absorptivities are approximately equal, and thus a simple optical absorption measurement can be used to determine the emissivity. In order to prove this, we can define the photon flux at an energy,  $e$  by

$$L'_x(e, \mu, T_0) = \frac{L_x(e, \mu, T_0)}{e\epsilon(e)}. \quad (2)$$

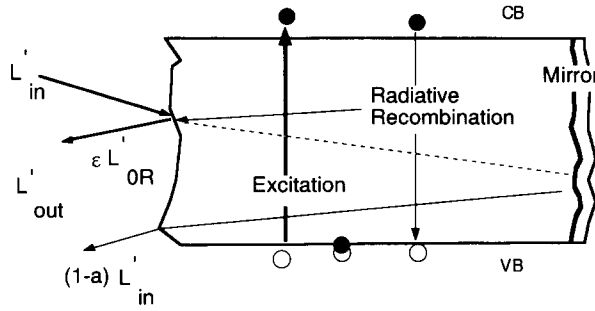


Fig. 2. A schematic energy diagram showing the balance between excitation by, and emission of, light. The output radiance always consists of the non-absorbed radiation plus the luminescence. If the input radiance equals the ambient black body radiation, an equilibrium occurs and the relation  $a = \epsilon$  can be demonstrated (see text).

One can then describe the output light,  $L'_{out}$ , from an absorber as the sum of the emitted luminescent light and the non-absorbed, i.e. reflected incident light for the geometry indicated in fig. 2. This gives [9]

$$L'_{out} = \epsilon(e)L'_{OR} + L'_{in}[1 - a(e)]. \quad (3)$$

If the incoming light is equal to the ambient blackbody radiation,  $L'_{in} = L'_{OR}$ , the chemical potential in eq. (1) is zero ( $L'_{OR} = L'_0$ ). The outgoing radiation must then balance the incoming, even in the presence of non-radiative losses. This means  $L'_{in}$  is equal to  $L'_{out}$ . For this case, eq. (3) yields

$$a(e) = \epsilon(e). \quad (4)$$

This equality is true since the absorption and emission are time reversible on a microscopic scale. Although we chose to evaluate the relationship between  $a$  and  $\epsilon$  at ambient equilibrium, these quantities are parameters that are characteristic of the absorber at a given temperature. If the incoming flux is not equal to the ambient radiation, then the chemical potential is not zero, and, from eq. (1), the radiative photon flux,  $L'_{OR}$ , is approximated by its ambient value,  $L'_0$ , multiplied by a Boltzmann factor of  $\exp(\mu/kT_0)$ . We have shown above that the radiative losses are given by  $a(e)L'_0$  under ambient radiation input, so that these losses are  $a(e)L'_0 \exp(\mu/kT_0)$  under solar illumination. Note that even though the probabilities given in eq. (4) are equal, the photon fluxes for the output or input, as given by eq. (1), will not always be equal. The input radiation is arbitrary, and the output luminescence is determined the chemical potential. In section 2.3, we will relate the chemical potential to the incoming flux, and photoluminescence efficiency.

The results given in eq. (4) allows one to easily evaluate eq. (1) from the absorptivity of a material. Fig. 3a shows the results of eq. (1) plotted for the ideal silicon luminescent spectrum using a voltage of 0.55 V, as well as the more realistic spectrum for silicon calculated by including the absorptivity,  $a(e)$ , shown in fig. 3b.

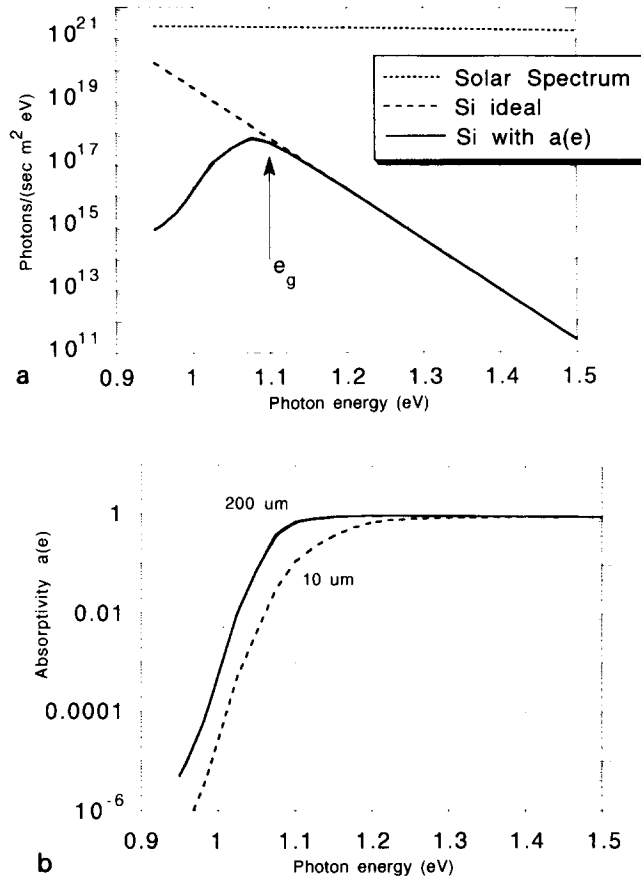


Fig. 3. (a) Photoluminescent spectrum of silicon at a temperature of  $T_0 = 300$  K. The chemical potential used is  $0.55$  eV in eq. (1). The solar spectrum is shown on the same log scale, and occurs at three orders of magnitude above the Si spectrum. The Si output is obtained by multiplying the ideal spectrum by the absorptivity,  $a(e)$ , for  $200 \mu\text{m}$  thick Si. (b) Calculated absorptivity–emissivity,  $a(e)$ , of a  $200 \mu\text{m}$  thick slab of silicon. The calculation utilized the Yablonovitch light trapping and absorption enhancement model [8] (see text). A thinner Si absorber, shown as a dashed line, would produce a more gradual transition from low to high photon energies.

The expected Si spectrum is thus obtained as the product of the absorptivity,  $a(e)$ , and the ideal spectrum, which is shown as a dotted line in fig. 3a. The absorptivity can be directly measured, or it can be calculated from the absorption coefficient. The absorptivity for a thick ( $t = 200 \mu\text{m}$ ) silicon slab was obtained from the absorption coefficient,  $\alpha(e)$ , shown in fig. 4, utilizing the light absorption and light trapping model of Yablonovitch [8]. This light absorption model has been shown to describe thin absorbers better than the Beer–Lambert law. This is because

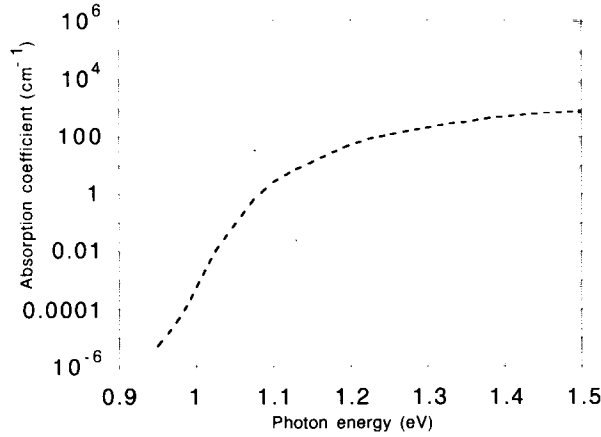


Fig. 4. Absorption coefficient of single crystal silicon, Si, used to calculate the absorptivity in fig. 3b [1,3,8].

multiple reflections, absorption enhancement, and light scattering are considered. In the case of maximum absorption, the absorptivity is thus given from the thickness,  $t$ , and the absorption coefficient as [8]

$$a(e) = \frac{\alpha(e)}{n^2\alpha(e) + 1/4t}. \quad (5)$$

In this paper, we shall assume that the transmission of the front, or illuminated, interface shown in figs. 1 and 2 is unity, and that the back surface of the absorber is a perfect mirror. This is a reasonable assumption for textured surfaces where light trapping occurs. For other cases, non-unity transmission coefficients can simply multiply eq. (5).

The peak in the photoluminescence spectrum in fig. 3a for silicon is shifted to an energy which is slightly lower than the optical bandgap energy ( $e_g = 1.1$  eV for Si). Silicon is only used here as an example. A similar result could be obtained for LED materials such as AlGaAs, or InGaAsP. The idealized solar spectrum utilized in this paper is shown in fig. 3a for comparison, and in figs. 5a and 5b on a linear plot. A reduced black body ambient curve is also shown in fig. 5a on the same scale. It can be seen from these curves that the solar flux level is approximately three orders of magnitude higher than the luminescent flux level from silicon, at 0.55 V, and that the ambient curve has a peak value that is two orders from the diluted solar spectrum. The peak wavelength of 1.07–1.08 eV and the shape of the Si photoluminescence spectrum shown in fig. 3a was confirmed experimentally and also found in the literature [14].

### 2.3. Relationship between voltage and luminescence efficiency

From eq. (1), it is possible to obtain the photoluminescent efficiency. For a slab of absorber material, at open circuit, OC, this luminescence efficiency,  $\Phi$ , is simply

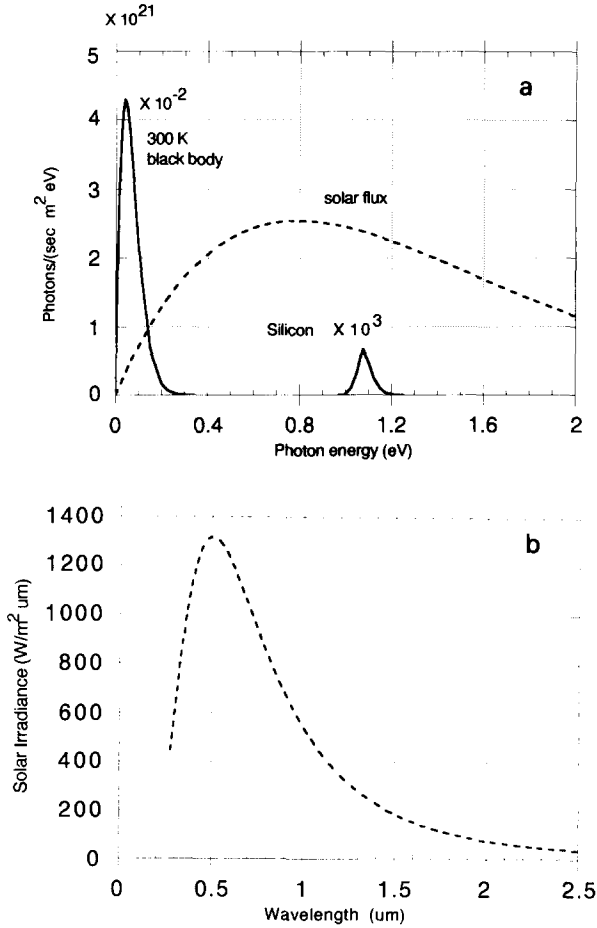


Fig. 5. Solar spectrum approximated by a diluted black body by setting the temperature  $T_0 = T_S = 5762$  K, and  $\mu = 0$  in eq. (1). This spectrum is calculated from the generalized Planck equation, eq. (1), multiplied by  $1.6 \times 10^{-5}$  to obtain an illumination at the earth's surface of  $1000 \text{ W/m}^2$ . The plots shown are for: (a) solar photon flux together with the  $T_0 = 300$  K black body flux, solid line, and (b) recalculated for the solar spectral irradiance as a function of wavelength.

the rate of photons emitted from the material,  $I_{0R}$ , divided by the incident photons absorbed,  $I_{SC}$ , plus the thermal excitations,  $I_0/\Phi$ . This involves a simple integration of eq. (2) over energy. Thus,

$$\Phi_{OC}(\mu, T) \equiv \Phi = \frac{I_{0R}}{I_{SC} + I_0/\Phi} = \frac{\text{radiative recombination}}{\text{total recombination}}. \quad (6a)$$



Solving this for  $\Phi$  yields

$$\Phi = \frac{\int_0^\infty \epsilon(e) \pi L'_{0R}(e, \mu) de - \int_0^\infty \epsilon(e) \pi L'_0(e) de}{D \int_0^\infty a(e) \pi L'_S(e) de}, \quad (6b)$$

where  $D$  is the dilution factor,  $1.6 \times 10^{-5}$  for  $1000 \text{ W/m}^2$ , which represents the inverse square fall off of the irradiance from the sun's luminous surface to the earth ( $0 < D < 1$ ) [5]. For most cases, the lower limit of the integration can be taken near  $e_g$ . The denominator in eq. (6b) is then the absorbed solar photon flux. If laser, or other light, is used instead of solar illumination, the denominator in eq. (6b) is replaced by the absorbed photon flux, per unit area, producing excited states. As an aside, if electroluminescence [1] is used instead of the photoluminescence, as for a light emitting diode, the denominator is replaced by the number of electrons per unit area injected into the CB, as current  $I$ . More will be said about the LED and current extraction in section 3.3. In the numerator of eq. (6b), the term subtracted is the small background black body flux at ambient temperature. This yields the net recombination due to the illumination or excess charge carrier density. The factor of  $\pi$  included in each integral is due to the integration over the projected solid angle [5,13]. In a more compact form, eq. (6b) becomes

$$\Phi = \frac{I_{0R} - I_0}{I_{SC}} \approx \frac{I_0 \exp(\mu/kT_0) - I_0}{I_{SC}}, \quad (6c)$$

where the terms in eq. (6c) are defined by eq. (6b). The approximation given in eq. (6c) consists of the Wien approximation of the generalized Planck equation given in eq. (1) (i.e.  $-1$  in the denominator of eq. (1) is neglected). The Wien approximation can also be used to obtain an approximate expression for the ambient photon current,  $I_0$ . Assuming an absorptivity of 1, the integration yields

$$I_0 = \frac{2\pi n^2}{h^3 c^2} (kT_0)^3 [\exp(-x_g)] (2 + 2x_g + x_g^2) \quad (7)$$

for the second integral in the numerator of eq. (6b), where  $x_g = e_g/kT_0$ . A similar expression is obtained for  $I_{SC}$ , where  $kT_S$  (0.4966 eV) replaces  $kT_0$  [5]. This expression applies if the absorptivity is a step function at the bandgap energy ( $a(e) = 1$  for  $e > e_g$ ). For most semiconductors, the first two terms in the parentheses can be neglected. In general, and especially for thin absorbers, the absorptivity is a function of the photon energy and the integrals in eq. (6b) must be carried out numerically. It is therefore worth noting from fig. 5a that if defects are present in the absorber such that they cause absorption near 0.05 eV, these defects will dramatically increase  $I_0$  and lower the voltages. More will be said about this in section 3.7. This may explain why intrinsic absorber and p-i-n structures yield higher measured voltages than doped material [1,2].

As stated previously, the quantum absorptivity and emissivity given in eq. (6b) are equal. This allows one to evaluate the results of eqs. (6b) and (6c). For

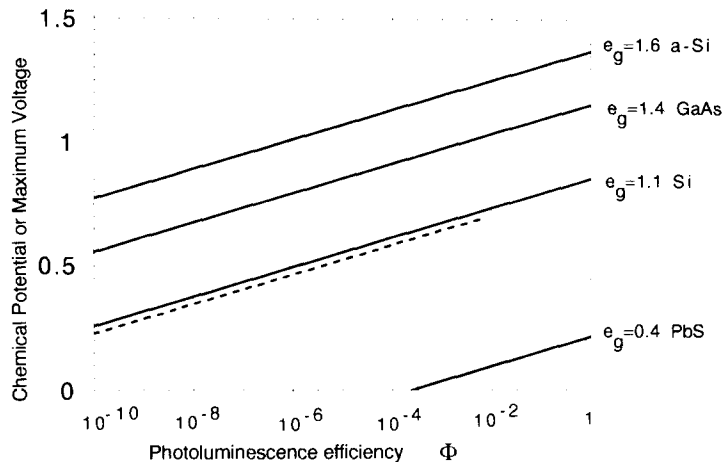


Fig. 6. Calculated voltage as a function of photoluminescence efficiency, under solar spectrum illumination, for various semiconductor materials using eq. (6c). The dashed curve for silicon utilizes the  $t = 200$   $\mu\text{m}$  data for the absorptivity,  $a(e)$ , in fig. 3b. The other materials utilize a step function absorptivity at the optical band gap,  $e_g$ , and eq. (7).

convenience, the radiance of the sun and ambient radiation,  $L_S$  and  $L_0$  respectively, are approximated as diluted black body radiation by setting  $\mu = 0$  and  $T_S = 5762$  K, or  $T_0 = 300$  K in eq. (1). This neglects atmospheric absorption, however, the results are essentially unchanged. Fig. 6 shows the results of eq. (6b) for various bandgap energies, assuming a step function absorptivity emissivity. Eq. (7) was thus used for the evaluation of  $I_{SC}$  and  $I_0$ . A photoluminescence efficiency,  $\Phi$ , of 1.0 represents 100% conversion and Stokes shifting of the incident light into re-emitted light. As can be seen, a logarithmic dependency of  $V_{OC}$  on  $\Phi$  is found. Shown as the dashed line in fig. 6 are the results of a numerical integration of eq. (6b), using the absorption data for silicon shown in figs. 3b and 4. The effect of this is the lower the “effective” bandgap of silicon from the 1.1 eV usually quoted. The results are in good agreement with experimental voltage values [1,3,15,16]. The experimental  $\Phi$  values for GaAs and Si are near  $10^{-1}$  and  $10^{-4}$ , respectively [1,14,17]. The voltages predicted from fig. 6, 1 V and 0.6 V, respectively, are in good agreement with observed values for 1 sun illumination. This is an important test for the model. In general, the voltage determined by eq. (6c) is slightly higher than the potential at the contacts due to resistive losses.

### 3. Discussion and alternative derivations

#### 3.1. Maximum open circuit voltage in a quantum device

The dependency of the open circuit voltage on the luminescent efficiency can be further emphasized by solving for the chemical potential in the approximation

given in eq. (6c). This allows one to obtain

$$qV_{OC} = \mu \approx kT_0 \ln(I_{SC}/I_0) + kT_0 \ln \Phi, \quad (8)$$

where  $I_{SC}$  is the short circuit, SC, current, and  $I_0$  becomes the ideal or lowest reverse saturation current for a given material. This is similar to the result originally obtained by Shockley and Queisser and others, except for the term containing  $\Phi$  [5–9]. This equation has the form of the usual diode equation with a correction for non-unity photoluminescence efficiency [1]. It is seen from eq. (8) and fig. 6 that a small photoluminescence efficiency, on the order of  $10^{-3}$  to  $10^{-4}$ , is sufficient for fairly efficient operation as a photovoltaic cell. The measured value of  $\Phi$  for silicon is in this range [7,8,14]. This correctly accounts for the voltages observed.

### 3.2.1. Alternative derivation using detailed balance

Eqs. (6) and (8) can be interpreted in terms of recombination and charge collection. This is obtained from the detailed balance of electrons in the conduction band (or excited state) shown in fig. 1. We will neglect resistive losses at present, but will discuss them in the section that follows. If we represent the ratio of the non-radiative recombination flux to radiative flux,  $I_{0R}$ , as  $\kappa$ , we obtain

$$\kappa = (\text{non-radiative losses})/(\text{radiative losses}). \quad (9a)$$

From eq. (6a), note that,

$$1 + \kappa = 1/\Phi. \quad (9b)$$

The parameter  $\kappa$ , like  $\Phi$ , is not a constant for the material, i.e. GaAs, Si, but is also dependent on the sample quality and defect concentration. For a given sample, however, it can be considered a constant. This allows one to balance electrons entering and leaving the excited state. Figs. 7a and 7b illustrate the relationship between the various losses. In fig. 7a, one sees that the solar and ambient photon fluxes produce an output current after radiative and non-radiative recombination have reduced the flow. This yields the balance

$$\begin{aligned} &\text{thermal excitations} + \text{ambient absorbed} + \text{solar absorbed} \\ &= \text{luminescent photons} + \text{phonons} + \text{current extracted}, \end{aligned} \quad (10a)$$

or

$$(\kappa + 1)I_0 + I_{SC} = I_{0R} + \kappa I_{0R} + I, \quad (10b)$$

where  $I$  is the current collected, per unit area, in the external circuit as shown in figs. 1 and 7b. The terms in eq. (10b) are defined by eqs. (6b) and (6c). The recombination flux or current is, from eq. (1), related to the voltage or chemical potential. In general, for a current extracted  $I$ , one obtains from eq. (10b)

$$I = I_{SC} - \frac{I_0}{\Phi} [\exp(\mu/kT_0) - 1]. \quad (10c)$$

This has the form of the well known diode equation [1,3,5]. If the electrical current density is desired, then the right hand side of eq. (10c) is multiplied by the

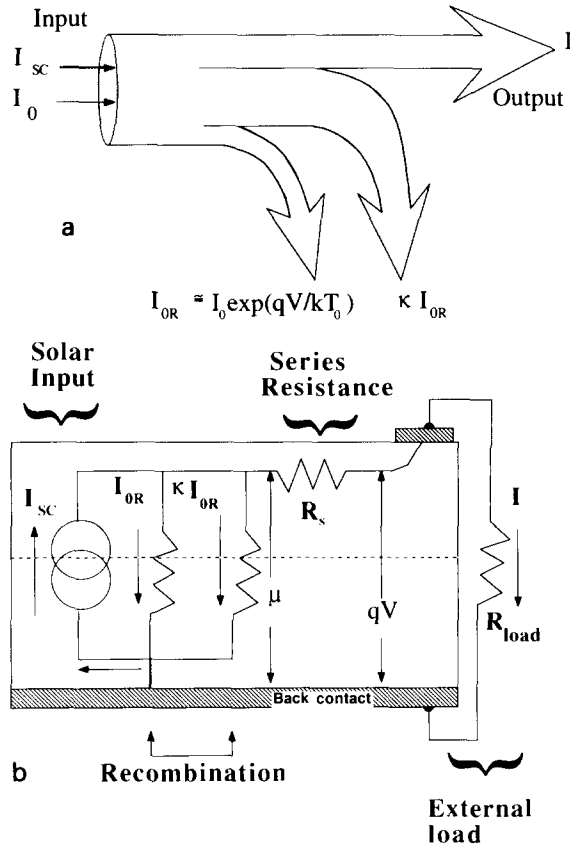


Fig. 7. (a) Schematic diagram showing the flow of current through a solar converter material. Solar, and a small flux of ambient blackbody radiation, enters the converter. What is left after recombination is present as a photocurrent,  $I$ . The radiative recombination, or loss, is given by  $I_{OR}$  and the non-radiative loss is given by  $\kappa I_{OR}$ . (b) Circuit diagram of a solar cell illustrating the relationship between the maximum voltage or chemical potential,  $\mu$ , series resistance, and the voltage appearing across the load resistor,  $R_{load}$ . The ratio of the non-radiative path to radiative, or luminescent, is  $\kappa$ .

elemental charge,  $q$  ( $1.6 \times 10^{-19}$  C/particle). Under open circuit conditions,  $I = 0$ , and eq. (10b) yields eqs. (6c) and (8). Comparing eq. (10c) to the diode equation [1],  $I_0/\Phi$  becomes the reverse saturation current, for the  $I-V$  curve. From eq. (7), the  $I_0$  value for Si is on the order of  $10^{-16}$  A/cm<sup>2</sup>. The best reverse saturation currents for Si diodes are near  $10^{-12}$  A/cm<sup>2</sup>. This confirms that the  $\Phi$  value is on the order of  $10^{-3}$ – $10^{-4}$  for Si, and lends validity to the recombination model represented by eqs. (6) and (10). The current-voltage characteristics of Si, under 1 sun illumination, are plotted in fig. 8. Photoluminescence measurements can thus predict the  $I-V$  curve of an optoelectronic device.

Eq. (10) can be understood as the balance between driving force, represented by  $\mu$ , and kinetic or rate processes represented by the current  $I$ . As the current

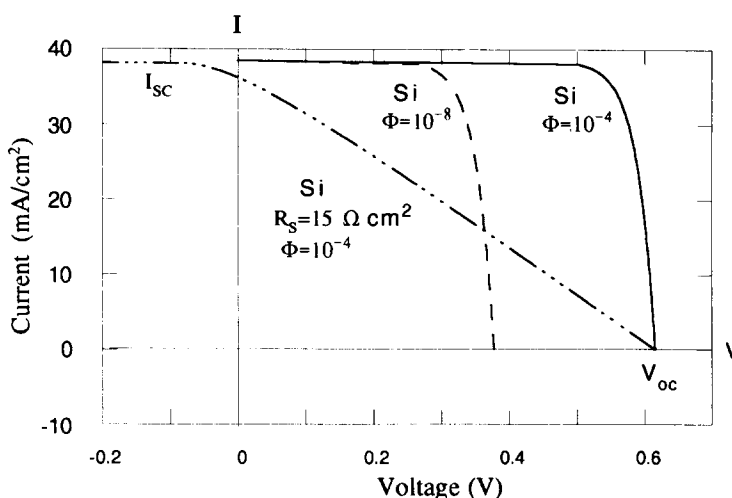


Fig. 8. Current voltage characteristic ( $I$ - $V$  curve) for an solar illuminated silicon converter, or diode, calculated utilizing the luminescence model and eq. (13). The nominal condition represents a Si photoluminescence efficiency of  $\Phi = 10^{-4}$ . The other two curves represent the effect of a series resistance,  $R_s = 15 \Omega$  for  $\Phi = 10^{-4}$ , and a lowering of luminescence with  $R_s = 0 \Omega$ , and  $\Phi = 10^{-8}$ .

extracted increases, the observed voltage, and thus luminescent and non-radiative flux, will decrease (i.e.  $\Phi$  and  $\kappa$  are constant). This is seen by comparing eqs. (1) and (10c). Solving eq. (10c) for the luminescence efficiency  $\Phi$  one obtains an expression that is identical to eq. (6c), with the exception that the denominator in eq. (6c) is replaced with  $I_{SC} - I$ , so that  $\Phi$  remains a constant for the sample. In other words, if a current is extracted, the *observed* photoluminescence efficiency will be that given by eq. (10b) multiplied by  $1 - n_i$ , where  $n_i$  is the fraction of  $I_{SC}$  extracted in the load [8]. This lowering of the luminescence with current the extracted, or chemical species produced, is observed experimentally in semiconductors [17]. It is also well known that the photoluminescence of chlorophyll is approximately 3% in a living plant, and 30% if the pigment is separated from the rest of the electron transport chain [4]. This corresponds to operation under load and open circuit, respectively.

### 3.2.2. Relationship to past work

The use of detailed balance and black body radiation to describe the efficiency of a solar cell, or quantum converter, is by no means new. The original paper by Shockley and Queisser [6] was followed by many others [7-9]. Chemical potential has also been included in the description of luminescence from semiconductors in the work of Würfel [12]. Würfel has included the concept of absorptivity in the description of the luminescence, similar to eq. (1), and found that this accurately described GaAs LED emission. The inclusion of non-radiative losses has been done by Ross, Yablonoitch and Baruch [7,8]. The concept of the effective temperature of the light has been used prior to that of the chemical potential [6].

In the present work, the concepts of luminescence, non-radiative recombination and chemical potential have been combined and presented in the nomenclature used in semiconductor device technology. The goal in this paper is to describe optoelectronic device parameters from simple measurements of the optical absorptivity and photoluminescence efficiency at room temperature. From the diode equation given by eq. (10c), it is shown how the photoluminescence efficiency, absorptivity and non-radiative recombination directly relate to the reverse saturation current. Applications and modifications of this approach will be presented in the sections that follow.

### 3.3. Application of the luminescence model to LEDs

The production of electricity from light implies a reverse process which is commonly used in the electronics industry [1]. This is the light emitting diode or LED. Referring to fig. 1, one can see that the injection of electrons into the conduction band from an external source, will increase the radiative, and non-radiative, recombination. In practice, charge injection is accomplished using a p-n junction identical to that used for solar cells. Since the photoluminescence efficiency of Si is very low, so too will be the electroluminescence [1]. For this reason, III-V materials such as AlGaAs and GaAsP are commonly used, since their photoluminescence yields lie in the range of  $10^{-2}$  to 1.0. The current-voltage curve presented in eq. (10c) is also applicable to LEDs. The illumination term,  $I_{SC}$ , can be neglected if the diode is not exposed to a light source. In general, the equations presented in this paper are applicable to LEDs, detectors, electroluminescent displays, and a variety of other optoelectronic devices.

A recent development for silicon will allow for an interesting application of the ideas presented in this paper [18,19]. It has been found that silicon can be made to yield visible photoluminescence and electroluminescence if it is first electrochemically etched in acid and then anodically oxidized to produce small, "quantum sized", columns of Si material. It is thought that the confinement of electrons in quantum-well-like structures allows for direct bandgap type behavior, and lower non-radiative losses. A p-type Si wafer treated in this way shows visible red-orange luminescence when placed under a normal UV lamp. Visible red electroluminescence is also observed during the oxidation step. In this case, the photoluminescence efficiency,  $\Phi$ , and absorptivity,  $a(e)$ , have changed from their normal values, so that higher open circuit voltages are predicted, from eqs. (8) and (10), for porous Si than for normal Si. Since the resistance of the material is on the order of  $10^6 \Omega$ , the photocurrent may be low, similar to that of an organic dye solar cell [2]. The effects of ohmic resistance, and of other kinetic factors, on the observed photocurrents will be discussed in section 3.6.

### 3.4. Conversion efficiency

The actual conversion efficiency,  $\eta^*$ , for a solar quantum converter or detector can be calculated from a sum of absorbed input light minus the radiative and

non-radiative losses all multiplied by the chemical potential per particle, or voltage. The efficiency is then given by

$$\eta^* = \frac{\mu[(\kappa + 1)I_0 + I_{SC} - (\kappa + 1)I_{0R}]}{\text{input solar power}}. \quad (11)$$

From eq. (10), the term in the brackets rearranges to the extracted current. This yields

$$\eta^* = \frac{\mu \left( I_{SC} - \frac{I_0}{\Phi} [\exp(\mu/kT_0) - 1] \right)}{D \int_0^\infty \pi L_S(e) de}. \quad (12)$$

The maximum power point is defined from  $d(\mu I)/dV = 0$ . Eq. (12) thus provides an important check of the validity of the luminescence and recombination model described in this paper. The luminescence-recombination approach for the determination of efficiency given in eq. (12) is identical to the traditional method of finding the voltage and current,  $V_m$  and  $I_m$  at the maximum power point obtained from the  $I$ - $V$  curve given in eq. (10) [1]. Note, from eqs. (1) and (11), that as the ambient temperature increases, so too will the radiative losses,  $I_{0R}$ . The derivative of the voltage expression given in eq. (8) yields  $d\mu/dT \approx -(1/T)(e_g - \mu)$  if eq. (7) is used for  $I_0$ . This derivative, which is approximately  $-2$  meV/K for Si, is equivalent to that obtained using p-n junction theory [1,3]. This results in a lowering of the conversion efficiency with temperature in a manner that has previously been described [5,9]. The luminescence approach has also been used to determine the maximum conversion efficiency as a function of bandgap, or cut-off, energy. For the case of  $\Phi = 1$ , the conversion efficiency given in eq. (12) peaks at approximately 33% near a bandgap energy of 1.4 eV [6-9]. Figs. 6 and 8 show that lower  $\Phi$  values result in a lower voltage values. Lower  $\Phi$  values will thus shift the  $\eta^*$  versus  $e_g$  curve downward [7].

### 3.5. Thin film absorber materials

Eq. (10) can also be used to explain the high voltages observed in very thin film solar cells and sensitized materials [1,20]. One can see from eqs. (1) and (8) that an optimum thickness might be found so as to maximize the power. As the thickness or particle size of the absorber is decreased, the maximum voltage,  $V_{OC}$ , will increase, since total recombination fluxes are lowered. This is due to the lowering of  $\epsilon(e)$ , and thus  $I_0$ , for thin absorbers (see fig. 3b). This is shown in fig. 9a for silicon, used here as an example. The data in figs. 3 and 4 were used for the calculation shown in figs. 9a and 9b. The absorbed solar flux,  $I_{SC}$ , on the other hand, will decrease with decreasing absorber thickness. The solar conversion efficiency is the product of the maximum voltage and current multiplied by the fill factor [1,3]. This is equivalent to eq. (12). Since the fill factor usually has an upper limit near 0.7-0.9, the product  $I_{SC}V_{OC}$  is a measure of the maximum solar

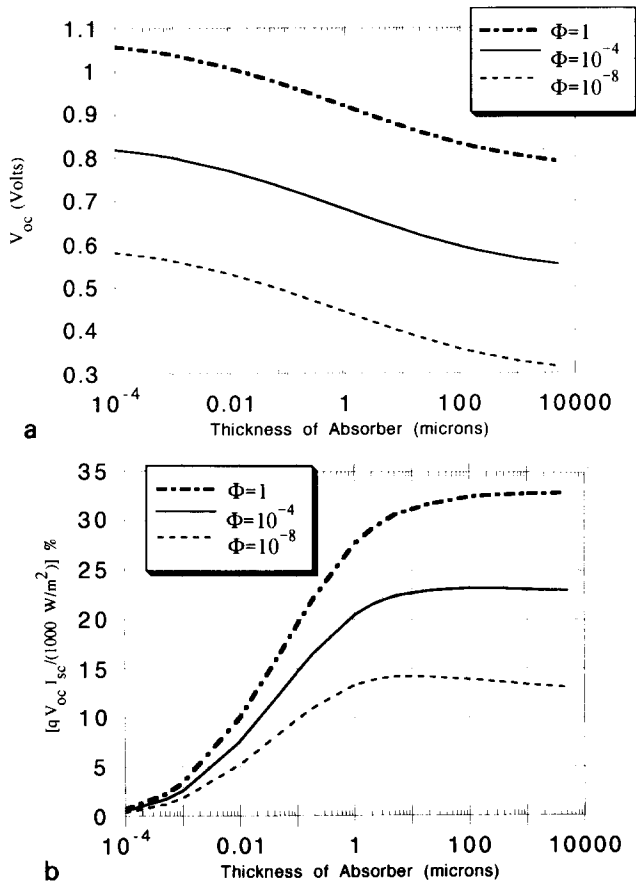


Fig. 9. (a) Maximum voltage,  $V_{OC}$ , versus thickness for silicon showing that higher voltages are predicted from eqs. (8) and (10c) for thinner absorber materials. The data in fig. 4 were used for the determination of  $a(e)$ . The photoluminescence efficiencies used are  $10^{-8}$ ,  $10^{-4}$ , and unity. (b) Normalized maximum current voltage product versus thickness for silicon under the same conditions as in (a). The curves should be truncated near  $5 \text{ \AA}$  for a one-atom thick Si layer.

conversion efficiency,  $\eta^*$ . This product,  $I_{SC}V_{OC}$ , is shown in fig. 9b for silicon, and attains an optimum for each photoluminescent efficiency value. A detailed optimization for silicon yielded similar results [8]. In contrast to the theoretical results shown in fig. 9a, as the absorber thinned, surface defect densities may dominate over bulk defects, and the value of  $\kappa$  may increase. This will limit the voltage values for small thickness values. It is experimentally known, however, that decreased thicknesses generally translate into higher output voltages [15,16]. The photoluminescence efficiency, and  $\kappa$ , as stated previously, are not constants for the material, but are dependent on the sample preparation, geometry and history. The example given in fig. 9 is only an illustration of the type of analysis possible using



the luminescence model. Silicon is used here as an example. Similar results may be found with any optoelectronic material. Thus, the thickness or particle size of an absorber should be such as to absorb most of the solar photons, but not as thick as to quench luminescence. Luminescence is thus seen as a loss to the process of conversion of light into useful work, but also as a measure of voltage and absorber material defect density. The higher the surface and bulk defect densities, the higher will be  $\kappa$ , the non-radiative recombination, and the lower will be the voltage  $\mu/q$ , the photoluminescence efficiency  $\Phi$ , and the conversion efficiency.

### 3.6. Resistive losses and kinetic effects

It should be noted from fig. 7b and eq. (12) that photoluminescence, though necessary, is not sufficient for an efficient solar cell or quantum converter. In this paper, the maximum voltage, chemical potential, or driving force has been described. Power is the product of driving force (thermodynamics) and flux (kinetics). Specifically, the photocurrents described in the equations presented in this paper must be supported by an adequate charge carrier mobility and conductivity of the material. Only then will photocurrent values near  $I_{SC}$  be realized in the external circuit. If a resistance  $R_S$  is included in series with the external load shown in fig. 7b, eq. (10c) is modified to

$$I = I_{SC} - \frac{I_0}{\Phi} \{ \exp[ q(V + qIR_S) / kT_0 ] - 1 \}. \quad (13)$$

The term in the numerator of the exponential factor represents the fact that the current is supported by the sum of the voltage generated, and the voltage drop across the contacts and bulk of the absorber material [1]. This is shown in fig. 7b. The series resistance is minimized by low loss contacts, higher mobility, and thinner absorber materials [1,3]. Fig. 8 shows the results of this equation plotted for various conditions for Si. Normal Si has a value of  $\Phi = 10^{-4}$ . This translates into a total reverse saturation current of  $2 \times 10^{-12}$  A/cm<sup>2</sup>. Series resistance decreases the power at the maximum power point, and the short circuit current and the fill factor. From fig. 8, note that when a lower luminescence efficiency is used, the maximum voltage is also lowered. This will also lower the conversion efficiency.

In addition, since the power is the product of the driving force and current, high electron collection quantum yields,  $\eta_q(e)$ , are required, *as well* as high  $\mu$  or  $V_{OC}$ , for efficient quantum solar converters [1]. The absorbed solar flux given from eq. 6 as  $I_{SC}$  may not all be available for the generated current shown in fig. 7b. This can be emphasized by examining the approximation for  $\eta_q(e)$  for a junction device given by [1,3]

$$\eta_q(e) \approx \frac{1}{1 + [1/\alpha(e)L_d]}, \quad (14a)$$

where

$$L_d = (kT_0 u \tau / q)^{1/2}. \quad (14b)$$

Here,  $\alpha(e)$  is the absorption coefficient, displayed for Si in fig. 4,  $L_d$  is the diffusion length, and  $u$  is the carrier mobility. The constant  $\tau$  is the carrier lifetime, which can be deduced from time resolved luminescence measurements [10,11]. The maximum current,  $I_{SC}$ , will then be estimated from the denominator of eq. 6b multiplied by  $\eta_q(e)$ . The current collection efficiency is usually near 0.9 unless the mobility is low [1–3]. This again illustrates that kinetics must work in tandem with thermodynamics to produce an efficient device. This aspect has been further emphasized by Archer and Bolton [21]. The average volume rate of radiative generation of charge carriers, in the dark, is  $I_0$  divided by the thickness,  $t$ , of the absorber. The volume rate of recombination in the dark has been shown to be a second-order rate constant multiplied by the equilibrium electron and hole concentrations [3,21]. From detailed balance, these two rates must be equal, and an expression for the radiative lifetime,  $\tau_{RS}$ , can thus be obtained (i.e. 1 ms for Si) [21]. This is the van Roosbroeck–Shockley lifetime. Non-radiative, and surface, recombination decrease the carrier lifetimes below this purely radiative value [1,3]. It has been shown, by Archer and Bolton, that if the lifetime is too short, the density of charge carriers generated in the light will not be able to support the maximum chemical potential potential,  $\mu_1$ , given by eq. (8) with  $\Phi = 1$  [21]. In this case, the equation

$$\mu = \mu_1 - kT_0 \ln(\tau_{RS}/\tau) \quad (15)$$

is obtained. Comparing this equation to eq. (8), one finds that the photoluminescence efficiency is the ratio of the actual carrier lifetime to the maximum value. Thus, short lifetimes, compared to the maximum radiative lifetime, are another way of expressing that the photoluminescence efficiency is low [1].

As an illustration of eqs. (14) and (15), organic dyes are known to have a photoluminescence efficiency near 1.0 [2]. Since the mobility of these materials is low and the resistivity,  $R_S$ , is high (i.e. poor kinetic factors) these materials produce high voltages, but show currents which are much lower than  $I_{SC}$ . Another illustration of the need of both high luminescence and mobility is pyrite,  $FeS_2$ . This semiconductor has been shown to possess a high absorption coefficient, and high  $I_{SC}$  values, as well as high electron collection quantum yields [22]. It has, however, shown no detectable photoluminescence down to a sensitivity limit of  $10^{-7}$  for  $\Phi$ . Photovoltages measured are lower than 200 mV when the pyrite is thick enough as required for these high  $\eta_q(e)$  values [22]. Since this material has an optical bandgap of 0.95 eV, this result is supported by eq. (10) and figs. 6 and 8. In contrast to organic dyes, pyrite shows good kinetic factors but poor thermodynamic properties. As shown in figs. 9a and 9b, thinner pyrite material may produce improved voltages, but these may be offset by lower currents unless light trapping can also be increased [8,23].

### 3.7. The diode quality factor

Up to now, only band to band recombination has been considered, and non-radiative processes have been represented through shallow defect levels, or through Auger processes (see fig. 1). If defects are present near the middle of the bandgap, recombination can occur via these defects levels. This will produce sub-bandgap photons for each recombination process. These photons, therefore, have a chemical potential which added together matches the chemical potential,  $\mu$ . One must then add an additional factor, of  $I_{02} \exp(\mu/AkT_0)$ , to the right side of eq. (10b) for recombination through these Shockley–Read-type centers [1,3]. This term also contains a photoluminescence efficiency term that describes the recombination process through these defect levels. A diode quality,  $1 < A < 3$ , factor thus accounts for emitted luminescent photons that are of sub-bandgap energies (see fig. 1). This additional term thus yields

$$I = I_{SC} - \frac{I_0}{\Phi} [\exp(\mu/kT_0) - 1] - I_{02} [\exp(\mu/AkT_0) - 1] \quad (16)$$

from eq. (10). An equation of this form is often used to describe the dark  $I-V$  curve of a p–n junction diode [1,3]. The evaluation of this additional term requires integration of eq. (2) utilizing the absorptivity at low photon energies (i.e. 0.5–0.05 eV). Within the framework of the luminescence model, light absorption at sub-bandgap energies is thus shown to increase recombination, and thus lower the maximum voltage (of course,  $I_{SC}$  may increase). The added term is dominant at low voltages, which are usually far from the operating voltage of a solar cell. For a well constructed diode these mid-gap defects are of low densities, and this additional recombination term is negligible [1,3].

Eqs. (16) and (14) seem to indicate that, for absorbers containing high defect densities, the value of  $\kappa$  or  $\Phi$  may be a function of the current and voltage conditions. This is, in fact, true, since various conditions may populate or depopulate defect levels. The luminescence model presented in this paper is a simple model intended to give fundamental insight into the factors that degrade performance. The voltages and currents represented by eq. (10) represent the maximum or ideal values. Further studies can reveal the variation of  $\kappa$  versus operating conditions and expand upon the model.

## 4. Conclusions

It has been shown that the photoluminescence of a material can be used to obtain an upper limit for the open circuit voltage of a quantum solar converter. In the future, therefore, it is desirable to obtain absolute photoluminescence, and absorptivity, measurements at room temperature, where the materials are used for solar energy conversion. Measurements at cryogenic temperatures will yield information on the nature of defects, but not necessarily on how they effect performance at 300 K. These measurements can yield information on process control and

material conversion efficiency [10,11]. Materials with reasonable photoluminescence quantum efficiencies are candidates for efficient optoelectronic devices. Although the concepts of luminescence have been applied specifically to solar conversion in this paper, these results are general. They have been applied to the study of solar concentrators, thermal converters, and optoelectronic devices such as lasers, and light emitting diodes [5,12,13,24]. Utilizing the concepts of photoluminescence in the study of solar energy may result in a brighter future for this energy source.

### Acknowledgements

The authors are indebted to Dr. Eli Yablonovitch of Bellcore for the stimulus for this work, and to Dr. Helmut Tributsch of the Hahn Meitner Institute for suggesting that kinetics be considered. The authors wish to thank Dr. Detlev Herm and Dr. Eychmüller of the Hahn Meitner Institute for their measurements of the photoluminescent properties of Si and chlorophyll.

### References

- [1] S.M. Sze, *Physics of Semiconductor Devices* (Wiley, New York, 1981) ch. 12, 14.
- [2] M. Hiramoto, H. Fujiwara and M. Yokoyama, *Appl. Phys. Lett.* 58 (1991) 1062.
- [3] C. Hu, R.M. White, *Solar Cells – From Basics to Advanced Systems* (McGraw-Hill, New York, 1983).
- [4] E. Rabinowitch, *Photosynthesis* (Wiley, New York, 1969).
- [5] R. Sizman, C. Winter and L. Vant Hull, *Solar Power Plants* (Springer, Berlin, 1991).
- [6] W. Shockley and H.J. Queisser, *J. Appl. Phys.* 32 (1961) 510;  
A. De Vos, *J. Phys. Chem. Solids* 49 (1988) 725.
- [7] R.T. Ross and J. Collins, *J. Appl. Phys.* 51 (1980) 4504;  
P. Baruch, *J. Appl. Phys.* 57 (1985) 1347.
- [8] T. Tiedje, E. Yablonovitch, G. Cody and B. Brooks, *IEEE Trans. Electron Devices* ED-31 (1984) 711;  
E. Yablonovitch and G. Cody, *IEEE Trans. Electron Devices* ED-29 (1982) 300.
- [9] A.F. Haught, *Physics Considerations of Solar Energy Conversion*, UTRC80-0 (United Technologies Research Center, East Hartford Connecticut, 1980); *J. Solar Energy Eng.* 106 (1984) 3.
- [10] J.W. Orton, P. Blood, *The Electrical Characterization of Semiconductors: Measurements of Minority Carrier Properties* (Academic Press, San Diego, 1990).
- [11] A. Mitchell and R. Gottscho, *Appl. Phys. Lett.* 56 (1990) 821.
- [12] H. Ries and A. McEvoy, *J. Photochem. Photobiol. A: Chem.* 59 (1991) 11;  
P. Würfel, *J. Phys. C: Solid State Chem.* 15 (1982) 3985.
- [13] G. Smestad, H. Ries, R. Winston and E. Yablonovitch, *Solar Energy Mater.* 21 (1990) 99.
- [14] L.T. Canham, *J. Phys. Chem. Solids* 47 (1986) 363.
- [15] A.W. Blakers and H.J. Queisser, in: *10th European Photovoltaic Solar Energy Conference*, Lisbon, Portugal, April 1991 (Kluwer, Dordrecht, 1991).
- [16] R.J. Schwartz and G.B. Turner, in: *10th European photovoltaic Solar Energy Conference*, Lisbon, Portugal, April 1991 (Kluwer, Dordrecht, 1991).
- [17] A. Burk, P. Johnson, W. Hobson and A. Ellis, *J. Appl. Phys.* 59 (1986) 1621.
- [18] A. Halimaoui, C. Oules and A. Bsiesy, *Appl. Phys. Lett.* 59 (1991) 304.
- [19] K.W.J. Barnham, B. Braun, C. Button and C.T. Foxon, *Appl. Phys. Lett.* 59 (1991) 135.

- [20] R. Vogel, K. Pohl and H. Weller, *Chem. Phys. Lett.* 174 (1990) 241.
- [21] M. Archer and J. Bolton, *J. Phys. Chem.* 94 (1990) 8028;  
J. Bolton and M. Archer, *J. Phys. Chem.* 95 (1991) 8453.
- [22] M. Birkholz, S. Fiechter, A. Hartman and H. Tributsch, *Phys. Rev. B* 43 (1991) 11926.
- [23] A. Luque and J. Minano, *Solar Cells*, 31 (1991) 237.
- [24] H. Ries, G. Smestad and R. Winston, in: *SPIE Proceedings 1528*, San Diego USA, July 1991.